Published in final edited form as:
Epilepsia. 2013 August ; 54(8): 1381–1390. doi:10.1111/epi.12199.

Automatic Detection of Primary Motor Areas Using Diffusion MRI Tractography: Comparison with Functional MRI and Electrical Stimulation Mapping

Jeong-Won Jeong[1,2,6], **Eishi Asano**[1,2], **Erik C. Brown**[4,5], **Vijay N. Tiwari**[1,2,6], **Diane C. Chugani**[1,3,6], and **Harry T. Chugani**[1,2,3,6]

[1]Carman and Ann Adams Department of Pediatrics, Children's Hospital of Michigan, Detroit, MI, USA

[2]Department of Neurology, Children's Hospital of Michigan, Detroit, MI, USA

[3]Department of Radiology, Children's Hospital of Michigan, Detroit, MI, USA

[4]Department of Psychiatry and Behavioral Neurosciences, Children's Hospital of Michigan, Detroit, MI, USA

[5]MD-PhD Program, Children's Hospital of Michigan, Detroit, MI, USA

[6]School of Medicine, Wayne State University Translational Imaging Laboratory, Children's Hospital of Michigan, Detroit, MI, USA

Summary

Purpose—As an alternative tool to identify cortical motor areas for planning surgical resection of children with focal epilepsy, the present study proposed a maximum *a posteriori* probability (MAP) classification of cortico-spinal tract (CST) visualized by diffusion MR tractography.

Methods—Diffusion weighted imaging (DWI) was performed in 17 normally developing children and 20 children with focal epilepsy. An independent component analysis tractography combined with ball-stick model was performed to identify unique CST pathways originating from mouth/lip, fingers, and leg areas determined by functional MRI (fMRI) in healthy children and electrical stimulation mapping (ESM) in epilepsy children. Group analyses were performed to construct stereotaxic probability maps of primary motor pathways connecting precentral gyrus and posterior limb of internal capsule, and then utilized to design a novel MAP classifier that can sort individual CST fibers associated with three classes of interest, mouth/lip, fingers, and leg. A systematic leave-one-out approach was applied to train an optimal classifier. A match was considered to occur if classified fibers contacted or surrounded true areas localized by fMRI and ESM.

Key Findings—It was found that the DWI-MAP provided high accuracy for the CST fibers terminating in proximity to the localization of fMRI/ESM, 78%/77% for mouth/lip, 77%/76% for fingers, 78%/86% for leg (contact) and 93%/89% for mouth/lip, 91%/89% for fingers, 92%/88% for leg (surrounded within 2 cm).

Corresponding author: Jeong-Won Jeong, PhD Departments of Pediatrics and Neurology, Wayne State University School of Medicine PET Center, Children's Hospital of Michigan 3901 Beaubien Blvd, Detroit, MI, 48201 Phone: 313-993-0258 Fax: 313-966-9228 jeongwon@pet.wayne.edu.

Disclosure of Conflicts of Interest

The authors declare no conflict of interest. We confirm that we have read the Journal's position on issues involved in ethical publication and affirm that this report is consistent with those guidelines.

Significance—This study provides preliminary evidence that in the absence of fMRI and ESM data, the DWI-MAP approach can effectively retrieve the locations of cortical motor areas and underlying CST courses for planning epilepsy surgery.

Keywords

Automatic Detection; Primary Motor Cortex; Corticospinal Tract; Diffusion MRI Tractography; Presurgical Planning; Epilepsy

Introduction

Epilepsy is one of the most common neurologic disorders and restricts the quality of life in affected individuals (Hirtz et al., 2007). New cases of epilepsy are most prominent among children. Anti-epileptic drug therapy is effective in approximately two-thirds of cases, implying that one-in-three do not obtain good seizure control or have unacceptable side effects from medications. Surgery to remove epileptogenic brain tissues is a good option for children (and adults) whose seizures cannot be controlled with medications. One key to successful surgery is to determine the spatial relationship between the seizure focus and functionally important pathways such as primary motor areas controlling movement. The precise delineation and sparing of these areas prevents postoperative motor deficits.

The current gold standard for identifying primary motor areas in human brain is electrical stimulation mapping (ESM) which, however, is invasive and often not adequately sensitive in young children (Wyllie & Awad, 1991; Haseeb et al., 2007; Lesser et al., 2010). A noninvasive imaging technique using fMRI, that measures blood oxygen level dependent contrast while tasking motor functions, has demonstrated great promise as a viable alternative to ESM (Ruge et al., 1999; Schlosser et al., 1999; Roessler et al., 2005; Kho et al., 2007; de Ribaupierre et al., 2012) . Although fMRI has been widely used for preoperative planning and decision-making (Medina et al., 2005; Nimsky et al., 2005; Roessler et al., 2005; Kho et al., 2007; de Ribaupierre et al., 2012) , it is challenging to perform fMRI studies in infants and young patients with neurological conditions, who are uncooperative or unable to follow task instructions during the study (Berntsen et al., 2008; Rumpel et al., 2009; Grabski et al., 2011; Wengenroth et al., 2011). Furthermore, the fMRI technique is inherently unable to localize crucial white matter structures, which may be at risk for damage or resection during surgery.

Diffusion weighted imaging (DWI) is a powerful technique that requires only limited patient cooperation and may be used to investigate white matter tracts (Basser et al., 1994; Basser, 1995; Conturo et al., 1999; Mori et al., 1999; Basser et al., 2000; Mori et al., 2000), such as cortico-spinal tract (CST) which, if damaged, would result in deficits of contralateral motor function (Nimsky et al., 2005). However, none of the previous studies on clinical DWI have reported on cortico-bulbar tract (CBT) that is distinctly connected to the inferior precentral gyrus and primarily executes control of movement of the mouth/lip. The reason for this is presumably due to the intravoxel problem of multiple crossing fibers at a voxel making it difficult to track this pathway (Alexander et al., 2001; Kinoshita et al., 2005; Mikuni et al., 2007; Qazi et al., 2009; Singh and Wong, 2010). We have recently developed a new tractography method combining independent component analysis and ball-stick model (ICA +BSM tractography) in order to isolate separate diffusion tensors of CBT, CST, arcuate fasciculus, and superior longitudinal fasciculus from each other and from other fiber tracts. Compared with post-mortem histology, the ICA+BSM tractography achieved an accuracy of 92.2% for reconstruction of CBT/CST derived from clinical DWI data (Jeong et al., 2012). This new approach has been applied in the present study.

The goals of the present study were to compare primary motor areas of the ICA+BSM method with ones of fMRI and ESM. We hypothesized that the termination of CBT/CST pathways at the cortex delineated by the ICA+BSM tractography would be concordant with fMRI- and ESM-defined motor areas of 'mouth/lips', 'fingers', and 'ankle/leg'. In addition, group analyses of 'mouth/lip', 'finger', and 'leg' pathways were used to develop in-vivo stereotaxic probability maps of 'mouth/lip', 'fingers', and 'leg' motor areas. Based on the resulting probability maps, a maximum *a posteriori* probability (MAP) classifier (DeGroot, 1970) was designed to automatically predict individual CBT/CST pathways. Thereby, a systematic leave-one-out approach was employed to avoid a circular analysis in evaluating the performance of DWI-MAP classification. Likewise, the DWI-MAP classifier was tested to predict the pathways of "mouth/lip", "fingers", and "leg" in children with focal epilepsy. The prediction accuracy was compared with extra-operative ESM.

Methods

Study Subjects

Seventeen normally developing children (age: 10.0±3.3 years, 4.3-17.8 years, 9 boys) and twenty children with the diagnosis of focal epilepsy (age: 12.3±4.9 years, 2.4-17.1 years, 13 boys) having epileptic foci in the vincinity of rolandic region were investigated. All participants were right-handed. Among twenty children with focal epilepsy, nine children had abnormal MRI showing a structural lesion. Patients with focal epilepsy had no gross motor deficit. The patients were selected by using the following inclusion criteria: (i) a history of intractable focal epilepsy scheduled for extraoperative subdural ESM as part of presurgical evaluation at Children's Hospital of Michigan, Detroit, (ii) mapping of motor and sensory functions via ESM. The exclusion criteria consisted of: (i) presence of massive brain malformations (such as large perisylvian polymicrogyria or hemimegalencephaly which entirely eliminate the anatomical landmarks for the central sulcus and sylvian fissure; these patients undergo one-stage hemispherectomy without extraoperative electrocorticography (ECoG) recording in our institute. Patients with other lesions including focal cortical dysplasia, cortical tubers, brain tumor, gliosis, and inflammation were not excluded from the present study), (ii) history of gross motor deficit, and (iii) history of previous neurological surgery. All studies were performed in accordance with policies of the institution review board with written informed consent.

MRI Acquisition

MRI scans were performed on a 3T GE-Signa scanner (GE Healthcare, Milwaukee, WI) equipped with an 8-channel head coil and ASSET. DW-MRI was acquired with a multi-slice single shot diffusion weighted echo-planar-imaging (EPI) sequence at repetition time (TR) = 12,500ms, echo time (TE) = 88.7ms, field of view (FOV) = 24cm, 128×128 acquisition matrix (nominal resolution = 1.89mm), contiguous 3mm thickness in order to cover entire axial slices of whole brain using 55 isotropic gradient directions with b= 1000s/mm^2, one b=0 acquisition, and number of excitations (NEX)=1. Approximate scanning time for the this acquisition was about 12 minutes using double refocusing pulse sequence to reduce eddy current artifacts. For anatomical reference, three-dimensional fast spoiled gradient echo sequence (FSPGR) were acquired for each participant at TR/TE/TI of 9.12/3.66/400 ms, slice thickness of 1.2 mm, and planar resolution of 0.94×0.94 mm^2.

fMRI Protocol

Whole brain fMRI data were acquired from normally developing children using T2*-weighted EPI sequence at TR=2000ms, TE=30ms, matrix=64×64, FOV=24cm, thickness=4mm. For mapping primary motor areas, a single 1-second instruction, to move the lip/mouth, clench fingers, or flex ankle/leg, was visually presented every five seconds,

consisting of a 15-second block to localize the motor cortex for the face, finger, or leg of each side. We repeated this block ten times (a 150-second task for three body parts of each side). . The fMRI activations were recorded for mouth/lip, fingers, and ankle/leg motor areas of each hemisphere and utilized as a binary mask to sort out relative CBT/CST from DWI tractography.

Processing of fMRI data

Statistical Parametric Mapping (SPM) general linear model with hemodynamic response function was used to identify the voxels corresponding to the activations of lip/mouth, fingers, and ankle/leg movement tasks. Statistical inferences were carried out at $p < 0.05$ based on family wise error (FWE) p-value and at extent threshold > 10. The resulting activations in “mouth/lip”, “finger”, and “leg” areas were subsequently co-registered to b0 image to be used as ROIs that sort out corresponding CBT/CST pathways.

Electrical stimulation mapping (ESM) in patients with focal epilepsy

The children with epilepsy underwent subdural electrode placement as a part of the clinical management for medically-uncontrolled seizures. ESM was performed to localize eloquent cortex as part of clinical care during extraoperative electrocorticography recordings (Fukuda et al., 2008) by one of the co-authors (EA), who was blinded to the results of DWI-MAP classifier. Subdural electrodes (diameter: 4 mm; inter-electrode distance: 10 mm) were placed over the hemisphere containing the presumed seizure focus. All electrode plates were stitched to adjacent plates or the edge of dura mater, to avoid movement of subdural electrodes after intracranial implantation. Subdural electrode pairs (**supplementary Fig. 1 a**) were stimulated by an electrical pulse-train of 5-seconds maximum duration using pulses of 300 μsec duration and frequency of 50 Hz at the bedside. Initially, stimulus intensity was set to 3 mA. Stimulus intensity was increased from 3 to 9 mA in a stepwise manner by 3 mA increments until a clinical response or after-discharge on electrocorticography was observed (**supplementary Fig. 1 b**). When after-discharge without an observed clinical response or when neither clinical response nor after-discharge was induced by the maximally-intense stimuli, the site was designated ‘not proven eloquent’. When both clinical response and after-discharges occurred, another pulse-train of the same or 1 mA smaller intensity was used until either clinical response or after-discharge failed to develop. Finally, a site with a contralateral movement induced by stimulation, without after-discharges, was classified as the ‘primary motor area’ for a given body part. If clinically necessary, we stimulated each site with another neighboring site to determine whether one, the other or both gyri were responsible for the clinical response, but this strict approach was not feasible in some patients due to a clinical reason (e.g.: patient fatigue). In addition, we recognize that ESM may induce a false positive finding because of its propagation to the surrounding site (Ishitobi et al., 2000). Nonetheless, ESM still serves as the gold standard method to determine the primary motor cortex in patients with epilepsy.

To register ESM electrodes to MRI, planar X-ray images (lateral and anterior-posterior) were acquired with subdural electrodes in place for localization on the brain surface; three metallic fiducial markers at anatomically well-defined locations aided co-registration with anatomical MRI (i.e., FSPGR). A three-dimensional MRI brain surface image was created with electrode sites delineated (von Stockhausen et al., 1997; Muzik et al., 2007; Alkonyi et al., 2009). Registration accuracy was confirmed by intraoperative digital photographs showing *in situ* electrode locations (Asano et al., 2005; Nagasawa et al., 2010; Wu et al., 2011). Utilizing in-house imaging software (Muzik et al., 2007), electrodes were converted into spherical masks of 8mm diameter, with the center of each electrode sphere resting on the pial surface of the cortex. Only the voxels representing the interface of the gray matter and white matter inside of the 8 mm sphere were included in the final electrode mask to

represent the nearest possible fiber termination sites. Masks, in three-dimensional MRI space, of electrodes associated with primary motor functions served to indicate ESM localization of 'mouth/lip', 'fingers', and 'leg' areas on the white matter surface.

Whole brain tractography using ICA+BSM

Details of the ICA+BSM tractography are available in recent publications (Jeong et al., 2012). In brief, multiple tensors recovery using ICA+BSM was performed at voxels of fractional anisotropy > 0.15 to filter out voxels of cerebrospinal fluid and noise. For each voxel to survive, an eleven neighborhood window was applied to create a diffusion data matrix whose row vectors indicate diffusion weighted signals at every voxel of window. Total K_{opt} tensors ($1 \leq K_{opt} \leq 3$) were estimated in framework of Bayesian Information Criterion (Basser et al., 1994) by iterating two complimentary steps, hidden source decomposition using fast ICA (Basser, 1995) and multi-compartment ball-stick model (Conturo et al., 1999). The first eigenvectors of resulting K_{opt}-tensors were utilized for whole brain tractography where total 100 seeds were defined at every voxel of gray matter. The present study modified the conventional streamline tracking algorithm (Mori et al., 1999; Basser et al., 2000; Mori et al., 2000) to accommodate multiple orientations in voxels. At each seed trial tracking was started in the orientation of one fiber randomly selected among K_{opt}- fibers. Step size and turning angle threshold were set to 0.2 voxel width and 60°, respectively.

Construction of stereotaxic probability maps of primary motor areas using fMRI and DWI tractography

For each participant of healthy children, four classes of bilateral CBT/CST pathways including C_1: mouth/lip CBT, C_2: finger CST, C_3: leg CST, and C_4: other remaining CBT/CST were systemically sorted by applying two regions of interest to entire tracts obtained from whole brain tractography, region 1: primary motor areas determined by the gold standard (fMRI) and region 2: posterior limb of internal capsule. To minimize inter-operator variability, all motor areas were accordingly co-registered to b0 image and binary Montreal Neurological Institute (MNI) space atlas of posterior limb of the internal capsule (WFU PickAtlas available at http://fmri.wfubmc.edu/cms/software) was placed into native head space by applying the inverse of spatial deformation obtained between the subject's b0 image and MNI b0 template (Ashburner, 2007).

To construct sterotaxic probability maps of four CBT/CST pathways, $P(x,y,z|C_{i=1,2,3,4})$, the number of fibers intersecting a point (x,y,z) were counted from each of CBT/CST pathways, $C_{i=1,2,3,4}$. The resulting numbers were scaled by total summation in order to define the probability values of four pathways at a given point of (x,y,z). Finally, the $P(x,y,z|C_{i=1,2,3,4})$ was spatially normalized into MNI space and averaged across participants to define standard atlas of CBT/CST.

Implementation of DWI MAP classifier

Under equal priors for four classes, $C_{i=1,2,3,4}$, the present study assumes that a posteriori probability of a given fiber $f_j(x,y,z)$ to belong to a class $C_{i,}$, $P(f_j|C_i)$, is equal to an average value of $P(x,y,z|C_i)$ over the entire trajectory of $f_j(x,y,z)$.

$$P\left(f_j|C_i\right) = \frac{1}{N}\sum_x\sum_y\sum_z f_j(x,y,z)\,P(x,y,z|C_i) \quad [1]$$

where $P(x,y,z|C_i)$ represents a stereotaxic probability map of class C_i in native head space obtained via inverse spatial normalization of a standard atlas, $P(x,y,z|C_i)$ mapping from MNI b0 template to the subject's b0 image. The value of $f_j(x,y,z)$ is equal to a unit when fiber f_j

intersects a point (x,y,z). N indicates the total number of intersections. Since the present study assumes an equal prior of C_i for i=1,2,3,4, the argument of i having the maximum posteriori probability, $P(f_j|C_i)$, determines the class membership of a given fiber, f_j.

Comparison of DWI-MAP with fMRI and ESM

To avoid a circular analysis in evaluating the performance of DWI-MAP classification, the present study employed a systematic leave-one-out trial where *M*-whole brain tracts, $f_{j=1,2,...,M}$, of a single subject was classified into one of four classes, $C_{i=1,2,3,4}$, by instantaneous DWI-MAP classifier whose $P(x,y,z|C_{i=1,2,3,4})$ were learned on the remaining subjects in the same group. At each trial, the cortical points of individual fibers, f_j, in C_i defined functional areas of C_i determined by DWI-MAP. Areas of DWI-MAP were compared with their gold standard, fMRI activations for healthy control and ESM grid locations for children with focal epilepsy, with a match considered to occur if areas of DWI-MAP contacted and overlapped areas of the gold standard. Matches between the DWI-MAP and the gold standard were also assessed as a function of distance to estimate receiver operative curves. The borders of DWI-MAP areas were extended by 0.5cm, 1cm, 1.5cm, and 2cm to determine whether the number of matches changed (FitzGerald et al., 1997).

To assess how accurately DWI-MAP classification ($C_{i=1,2,3}$) localizes primary motor areas determined by fMRI and ESM, a percentage overlap approach was utilized (Ciccarelli et al., 2003). A fiber visitation map of C_i was created by counting the number of streamlines intersected per voxel (Catani et al., 2007). The resulting map was finally normalized to MNI space using the spatial deformation derived from the process of normalization of the b0 image, averaged across all subjects, and scaled by a value of maximum visitation in the map, which defined a percentage overlap map. The percentage overlap map of each C_i was compared with primary motor areas determined by the gold-standard (i.e., fMRI for healthy children and ESM for children with epilepsy) utilizing Receiver operating characteristic (ROC) curve analysis. Group average of accuracy, sensitivity, and specificity for $C_{i=1,2,3}$ were obtained from all possible leave-one-out trials.

$$accuracy=\frac{TP+TN}{TP+FN+FP+TN}$$
$$sensitivity=\frac{TP}{TP+FN} \qquad specificity=\frac{TN}{FP+TN}$$
$$\mathrm{TP}(\%)=\frac{\mathrm{V}(\mathrm{O}\cap\mathrm{G})}{\mathrm{V}(\mathrm{G})}\times 100, \quad \mathrm{TN}(\%)=\frac{\mathrm{V}(\mathrm{O}^c\cap\mathrm{G}^c)}{\mathrm{V}(\mathrm{G}^c)}\times 100 \qquad [2]$$
$$\mathrm{FP}(\%)=\frac{\mathrm{V}(\mathrm{O}\cap\mathrm{G}^c)}{\mathrm{V}(\mathrm{G}^c)}\times 100, \quad \mathrm{FN}(\%)=\frac{\mathrm{V}(\mathrm{O}^c\cap\mathrm{G})}{\mathrm{V}(\mathrm{G})}\times 100$$

where V represents the volume of a set; G and O denote binary masks that are obtained from the gold-standard and the percentage map of DWI-MAP, respectively; c indicates the complementary set. TP, TN, FP, and FN indicate true positive, true negative, false positive, and false negative, respectively.

Results

Tractography using fMRI based seed regions

The present study used fMRI data to create the seed regions used for the tractography for a given healthy subject. Both the single tensor based DTI and ICA+BSM tractography were seeded in the voxels of fMRI activations and sorted by two ROIs, posterior limb of internal capsule (magenta) and pons (gray) in the healthy subjects. **Supplementary figure 2** shows that more streamlines could be identified using the ICA+BSM compared to single-tensor based DTI. It is clear that the ICA+BSM was able to reconstruct different CST pathways propagating from different motor areas including mouth/lip, fingers, and legs.

Generation of stereotaxic probability maps

Group analysis of 'mouth/lips', 'fingers', and 'ankle/leg' pathways that were obtained from the healthy group using ICA+BSM was used to produce homunculus maps of 'mouth/lips', 'fingers', and 'ankle/leg' areas representing the probability of 'mouth/lip', 'finger', and 'leg' pathways (**Figure 1**). It was found that inferior-lateral pathways (mouth/lip) are more likely to be connected to anterior part of posterior limb of internal capsule (PLIC) while medial pathways (fingers, ankle/leg) are more likely to be connected to posterior part of PLIC, which is consistent with known neuroanatomical connections between precentral gyrus and PLIC (Bertrand et al., 1965; Hardy et al., 1979; Dawnay and Glees, 1986).

Performance analysis of the DWI-MAP classifier compared to the gold-standard

One of the key advantages of using the proposed MAP classifier is the ability to identify the CBT-CST pathways of "mouth/lips", "fingers", and "ankle/leg" whose cortical terminations indicate the exact locations of gray matter involved in the movement of a given body part. **Figure 2** shows three CBT-CST pathways, C_1: mouth/lip, C_2: finger, C_3: leg obtained using DWI-MAP classification of one healthy control who was left out from the group used to build the homunculus. It is clear that the proposed MAP classification detected three subsets of the CBT-CST pathways (blue: mouth/lip fibers, red: finger fibers, green: leg fibers) apparently terminating at three different fMRI localizations (yellow clusters). Although the ICA+BSM tractography produced some fibers which terminated outside the voxels of fMRI clusters, this example demonstrates that the MAP classifier can be used to detect locations of both gray matter and white matter involved in the movement of "mouth/lip", "fingers", and "leg" without the use of own fMRI cluster seeds.

The DWI-MAP classifications of four patients with focal epilepsy, C_1: mouth/lip, C_2: finger, C_3: leg, are presented in **Figure 3**. Compared with the "mouth/lip", "finger", and "leg" motor area determined by ESM, the DWI-MAP method successfully localized the lateral projections of CST fibers originating from the primary mouth/lip and hand areas in all patients, where localization of the motor pathways is important to minimize the risk of a post-operative motor deficit.

To assess how accurately the proposed DWI-MAP classification can detect the localizations of "mouth/lip", "finger", and "leg" areas determined by the gold-standard, the group percentage overlap maps of DWI-MAP were compared with those of the gold standard (**Figure 4**). The DWI-MAP showed the cortical areas of C_1: mouth/lip, C_2: finger, and C_3:leg, mainly localized at or near pre/post-central gyrus, which are apparently matched to those of the gold-standard, fMRI in healthy children and ESM in children with epilepsy.

The ROC plots of sensitivity, specificity, and accuracy of data are shown in **Figure 5**. Using leave-one-out cross validation, the sensitivity of the DWI-MAP classifier over fMRI combined across all normal children increased from 37% (mouth/lip), 59% (finger), 57% (leg) when the most stringent criterion (contact) was used to 98% (mouth/lip), 97% (finger), 99% (leg) when the 2 cm criterion was used. For children with epilepsy, sensitivity of the DWI-MAP over ESM increased from 36% (mouth/lip), 59% (finger), 60% (leg) to 94% (mouth/lip), 100% (finger), 100% (leg), respectively, as the criterion changed from 'contact' to '2 cm away from the centroid of the electrode'. Specificity of the DWI-MAP classifier across normal children decreased from 99% (mouth/lip), 98% (finger), 98% (leg) to 89% (mouth/lip), 84% (finger), 86% (leg) as the criterion was relaxed from contact to 2 cm from the tracts to the boundary of the fMRI activation. Similarly, specificity of the DWI-MAP classifier across epilepsy children decreased from 98% (mouth/lip), 96% (finger), 97% (leg) to 87% (mouth/lip), 80% (finger), 84% (leg) as the criterion was relaxed from contact to 2 cm from the tracts to the centroid of the electrode.

The DWI-MAP classifier showed accuracies of 78% (mouth/lip), 77% (finger), and 78% (leg) in normal controls and 77% (mouth/lip), 76% (finger), and 86% (leg) in epilepsy children when the contact criterion was applied. Higher accuracies were achieved at 93% (mouth/lip), 91% (finger), and 92% (leg) in normal children and 89% (mouth/lip), 89% (finger), and 88% (leg) in epilepsy children when the 2 cm criterion was applied.

Discussion

This diffusion MRI study is a preliminary examination of the clinical feasibility of a new fiber tractography technique for simultaneous localization of cortical areas of primary motor functions and their underlying white matter tracts for presurgical planning in children with intractable focal epilepsy. The study provides the promising method to localize the primary motor areas in clinical cases where neither fMRI nor ESM is easy to employ. The results obtained from this study have important implications for presurgical planning of infants or young children with focal epilepsy or other neurological conditions, without any extra cost of other imaging modalities.

The principle of presurgical evaluation for epilepsy is to determine the spatial relationship between the epileptogenic zone and functionally important cortex. Without accurate localization of such brain regions, one cannot accomplish the ultimate goal of epilepsy surgery, which is to eliminate the recurrence of epileptic seizures without creating new sensorimotor or cognitive deficits. The current gold standard to identify the motor cortex is direct ESM (Wyllie & Awad, 1991; Haseeb et al., 2007; Lesser et al., 2010). Yet, stimulation is not an ideal gold standard method, since it carries the inherent risk of electrically-induced seizures, and sometimes fails to identify the motor cortex in children (Haseeb et al., 2007). An alternative approach is fMRI, which is highly susceptible to movement artifacts and demands cooperation of the patient during scanning; thus, fMRI is difficult to apply to young children with epilepsy (Berntsen et al., 2008; Rumpel et al., 2009; Grabski et al., 2011; Wengenroth et al., 2011; de Ribaupierre et al., 2012). Since the epileptogenic zone sometimes involves the bottom of a deep sulcus (Besson et al., 2008), a functional brain mapping modality capable of identifying the origin and course of functionally important pathways is highly desirable.

To overcome the limitations of currently available motor mapping modalities, the present study hypothesized that a new diffusion tractography method called “ICA+BSM” can serve as a tool to accurately visualize CST projections to mouth/lip, finger, and ankle/leg motor areas. The present study examined the inter-subject variation (or reproducibility) of the ICA +BSM by introducing the homunculus representation of mouth/lip, finger, and leg pathways using clinical DWI with a small number of gradient directions and low b-value. The resulting homunculus maps of primary motor pathways were then applied to design an objective classifier that detects the CBT and CST pathways terminating at the cortices of mouth/lip, finger, and leg areas. The cortices at the origin of mouth/lip, finger, and leg pathways were finally compared with both fMRI and ESM findings. The results indeed demonstrated the reliability of ICA+BSM tractography as compared to noninvasive fMRI and invasive ESM.

A critical assumption of this approach is that no significant reorganization took place in the development of CST pathways in children with focal epilepsy, implying that the CST variability in children with focal epilepsy is within that in healthy controls. Also, the present study assumes that the end of CTS pathways should contain the motor cortex in children even with structural lesions. This critical assumption may limit the accuracy of DWI-MAP classifier in children with large lesions (such as hemimegalencephaly or perisylvian polymicrogyria) that may reorganize the CST. The current study is not designed to validate

the DWI-MAP classification in such extreme cases, which very rarely undergo extraoperative ECoG recording. Under the assumption that the end of CST pathways should contain the motor cortex, the DWI-MAP classification utilizes the conditional probability maps estimated from fMRI data of normal children. Although fMRI includes vascular in-flow artifacts providing low specificity (Schlosser et al., 1999), our preliminary results suggest that the fMRI driven conditional probability maps are effective to localize primary motor areas. The proposed DWI-MAP classifier achieved accurate localizations comparable to ESM. If sufficient cases are available, one could investigate how the performance of DWI-MAP classifier is affected by the size and location of pathological lesions or reorganization in patients with focal epilepsy.

Another major challenge to the present study was the potential error in registration of ESM and MRI to assess the accuracy of the proposed DWI-MAP classifier. To minimize inter-operator errors in registering ESM to MRI, future studies might use a new registration method based on surface warping algorithms. The sulcus and electrodes in a two-dimensional digital picture will be detected by applying a conventional active contour model and then registering to a sagittal plane of three dimensional rendered MRI using fast diffeomorphic landmark-free surface registration (Yeo et al., 2010). This registration scheme may ensure better localization using the DWI-MAP classifier with ESM based on the cortical homunculus map. Since the present study relies on *a priori* knowledge constructed from fMRI (or ESM), our DWI method may not able to detect deeper portions of the tract for which fMRI (or ESM) may be limited in detecting associated functions. Reduced accuracy for the tracts associated with the leg area may be caused by their deeper position, suggesting that the present approach may be effective only for cortical activation using fMRI or stimulation to the proximity/termination of tracts. It should be noted that large subdural electrodes cannot be placed on the medial surface of the Rolandic area due to the presence of large bridging veins; thus, lower accuracy in finding the leg motor areas may be partly attributed to sampling errors on the gold-standard ESM approach. Future studies should examine this effect more carefully with other potential confounds such as age, gender, and the scanner type itself.

In conclusion, a novel DWI-MAP classification using ICA+BSM showed promise to perform simultaneous localization of cortical areas and white matter pathways associated with important motor functions. This preliminary study demonstrated that our method objectively discriminated the lateral-medial CST pathways originating from mouth/lip, finger, and leg areas, which are clinically important to plan resective epilepsy surgery in patients with focal epilepsy, and further assess the degree of motor deficit associated with abnormal gray/white matter in patients with other neurological conditions. By combining DWI-MAP classification with fMRI and ESM, we present new insights as to how white matter tractography may be used to delineate lateral-medial CST pathways in patients who are uncooperative or not able to follow task instructions in clinical studies. In summary, the significance of the present study for presurgical planning in epilepsy patients includes: (i) no added risk, (ii) no requirement of patient cooperation, (iii) high sensitivity to identify the motor cortex even in young children, (iv) capability to trace the course of different motor pathways, and (v) may be useful for other types of neurosurgical procedures (i.e., tumor resection).

Supplementary Material

Refer to Web version on PubMed Central for supplementary material.

Acknowledgments

This study was partially funded by a grant from the National Institute of Health, (R01 NS064989 to H.C and R01 NS64033 to E.A.). We thank Rajkumar M. Gorvindan, M.D. for thoughtful discussion. The authors would like to thank all participants and their families for their time and interest in this study.

References

Alexander AL, Hasan KM, Lazar M, Tsuruda JS, Parker DL. Analysis of partial volume effects in diffusion-tensor MRI. Magn Reson Med. 2001; 45:770–780. [PubMed: 11323803]

Alkonyi B, Juhasz C, Muzik O, Asano E, Saporta A, Shah A, Chugani HT. Quantitative brain surface mapping of an electrophysiologic/metabolic mismatch in human neocortical epilepsy. Epilepsy Res. 2009; 87:77–87. [PubMed: 19734012]

Asano E, Juhász C, Shah A, Muzik O, Chugani DC, Shah J, Sood S, Chugani HT. Origin and propagation of epileptic spasms delineated on electrocorticography. Epilepsia. 2005; 46:1086–1097. [PubMed: 16026561]

Ashburner J. A fast diffeomorphic image registration algorithm. Neuroimage. 2007; 38:95–113. [PubMed: 17761438]

Basser PJ. Inferring microstructural features and the physiological state of tissues from diffusion-weighted images. NMR Biomed. 1995; 8:333–344. [PubMed: 8739270]

Basser PJ, Mattiello J, LeBihan D. MR diffusion tensor spectroscopy and imaging. Biophys J. 1994; 66:259–267. [PubMed: 8130344]

Basser PJ, Pajevic S, Pierpaoli C, Duda J, Aldroubi A. In vivo fiber tractography using DT-MRI data. Magn Reson Med. 2000; 44:625–632. [PubMed: 11025519]

Berntsen EM, Samuelsen P, Lagopoulos J, Rasmussen IA Jr. Haberg AK, Haraldseth O. Mapping the primary motor cortex in healthy subjects and patients with peri-rolandic brain lesions before neurosurgery. Neurol Res. 2008; 30:968–973. [PubMed: 18671900]

Bertrand G, Blundell J, Musella R. Electrical Exploration of the Internal Capsule and Neighbouring Structures during Stereotaxic Procedures. J Neurosurg. 1965; 22:333–343. [PubMed: 14318109]

Besson P, Andermann F, Dubeau F, Bernasconi A. Small focal cortical dysplasia lesions are located at the bottom of a deep sulcus. Brain. 2008; 131:3246–3255. [PubMed: 18812443]

Catani M, Allin MP, Husain M, Pugliese L, Mesulam MM, Murray RM, Jones DK. Symmetries in human brain language pathways correlate with verbal recall. Proc Natl Acad Sci USA. 2007; 104:17163–17168. [PubMed: 17939998]

Ciccarelli O, Toosy AT, Parker GJ, Wheeler-Kingshott CA, Barker GJ, Miller DH, Thompson AJ. Diffusion tractography based group mapping of major white-matter pathways in the human brain. Neuroimage. 2003; 19:1545–1555. [PubMed: 12948710]

Conturo TE, Lori NF, Cull TS, Akbudak E, Snyder AZ, Shimony JS, McKinstry RC, Burton H, Raichle ME. Tracking neuronal fiber pathways in the living human brain. Proc Natl Acad Sci USA. 1999; 96(18):10422–10427. [PubMed: 10468624]

Dawnay NA, Glees P. Somatotopic analysis of fibre and terminal distribution in the primate corticospinal pathway. Brain Res. 1986; 391(1):115–123. [PubMed: 3955378]

de Ribaupierre S, Fohlen M, Bulteau C, Dorfmuller G, Delalande O, Dulac O, Chiron C, Hertz-Pannier L. Presurgical language mapping in children with epilepsy: clinical usefulness of functional magnetic resonance imaging for the planning of cortical stimulation. Epilepsia. 2012; 53:67–78. [PubMed: 22126260]

DeGroot, M. Optimal Statistical Decisions. McGraw-Hill; 1970.

FitzGerald DB, Cosgrove GR, Ronner S, Jiang H, Buchbinder BR, Belliveau JW, Rosen BR, Benson RR. Location of language in the cortex: a comparison between functional MR imaging and electrocortical stimulation. Am J Neuroradiol. 1997; 18:1529–1539. [PubMed: 9296196]

Fukuda M, Nishida M, Juhasz C, Muzik O, Sood S, Chugani HT, Asano E. Short-latency median-nerve somatosensory-evoked potentials and induced gamma-oscillations in humans. Brain. 2008; 131:1793–1805. [PubMed: 18508784]

Grabski K, Lamalle L, Vilain C, Schwartz JL, Vallee N, Tropres I, Baciu M, Le Bas JF, Sato M. Functional MRI assessment of orofacial articulators: Neural correlates of lip, jaw, larynx, and tongue movements. Hum Brain Mapp. 2012; 33:2306–2321. [PubMed: 21826760]

Hardy TL, Bertrand G, Thompson CJ. The position and organization of motor fibers in the internal capsule found during stereotactic surgery. Appl Neurophysiol. 1979; 42:160–170. [PubMed: 380467]

Haseeb A, Asano E, Juhasz C, Shah A, Sood S, Chugani HT. Young patients with focal seizures may have the primary motor area for the hand in the postcentral gyrus. Epilepsy Res. 2007; 76:131–139. [PubMed: 17723289]

Hirtz D, Thurman DJ, Gwinn-Hardy K, Mohamed M, Chaudhuri AR, Zalutsky R. How common are the “common” neurologic disorders? Neurology. 2007; 68:326–337. [PubMed: 17261678]

Ishitobi M, Nakasato N, Suzuki K, Nagamatsu K, Shamoto H, Yoshimoto T. Remote discharges in the posterior language area during basal temporal stimulation. Neuroreport. 2000; 11:2997–3000. [PubMed: 11006982]

Jeong JW, Asano E, Yeh FC, Chugani DC, Chugani HT. Independent component analysis tractography combined with ball and stick model to isolate intra-voxel crossing fibers of the corticospinal tracts in clinical diffusion MRI. Magn Reson Med. 2012 Published online: 21-Sep-2012; doi:10:1002/mrm.24487.

Kho KH, Rutten GJ, Leijten FS, van der Schaaf A, van Rijen PC, Ramsey NF. Working memory deficits after resection of the dorsolateral prefrontal cortex predicted by functional magnetic resonance imaging and electrocortical stimulation mapping. J Neurosurg. 2007; 106:501–505. [PubMed: 17566410]

Kinoshita M, Yamada K, Hashimoto N, Kato A, Izumoto S, Baba T, Maruno M, Nishimura T, Yoshimine T. Fiber-tracking does not accurately estimate size of fiber bundle in pathological condition: initial neurosurgical experience using neuronavigation and subcortical white matter stimulation. Neuroimage. 2005; 25:424–429. [PubMed: 15784421]

Lesser RP, Crone NE, Webber WR. Subdural electrodes. Clin Neurophysiol. 2010; 121:1376–13792. [PubMed: 20573543]

Medina LS, Bernal B, Dunoyer C, Cervantes L, Rodriguez M, Pacheco E, Jayakar P, Morrison G, Ragheb J, Altman NR. Seizure disorders: functional MR imaging for diagnostic evaluation and surgical treatment--prospective study. Radiology. 2005; 236:247–253. [PubMed: 15987978]

Mikuni N, Okada T, Nishida N, Taki J, Enatsu R, Ikeda A, Miki Y, Hanakawa T, Fukuyama H, Hashimoto N. Comparison between motor evoked potential recording and fiber tracking for estimating pyramidal tracts near brain tumors. J Neurosurg. 2007; 106:128–133. [PubMed: 17236498]

Mori S, Crain BJ, Chacko VP, van Zijl PC. Three-dimensional tracking of axonal projections in the brain by magnetic resonance imaging. Ann Neurol. 1999; 45:265–269. [PubMed: 9989633]

Mori S, Kaufmann WE, Pearlson GD, Crain BJ, Stieltjes B, Solaiyappan M, van Zijl PC. In vivo visualization of human neural pathways by magnetic resonance imaging. Ann Neurol. 2000; 47:412–414. [PubMed: 10716271]

Muzik O, Chugani DC, Zou G, Hua J, Lu Y, Lu S, Asano E, Chugani HT. Multimodality data integration in epilepsy. Int. J. Biomed. Imaging. 2007; 2007:13963. [PubMed: 17710251]

Nagasawa T, Rothermel R, Juhasz C, Fukuda M, Nishida M, Akiyama T, Sood S, Asano E. Cortical gamma-oscillations modulated by auditory-motor tasks-intracranial recording in patients with epilepsy. Hum. Brain Mapp. 2010; 31:1627–1642. [PubMed: 20143383]

Nimsky C, Ganslandt O, Hastreiter P, Wang R, Benner T, Sorensen AG, Fahlbusch R. Preoperative and intraoperative diffusion tensor imaging-based fiber tracking in glioma surgery. Neurosurgery. 2005; 56:130–137. [PubMed: 15617595]

Qazi AA, Radmanesh A, O'Donnell L, Kindlmann G, Peled S, Whalen S, Westin CF, Golby AJ. Resolving crossings in the corticospinal tract by two-tensor streamline tractography: Method and clinical assessment using fMRI. Neuroimage. 2009; 47:T98–T106. [PubMed: 18657622]

Roessler K, Donat M, Lanzenberger R, Novak K, Geissler A, Gartus A, Tahamtan AR, Milakara D, Czech T, Barth M. Evaluation of preoperative high magnetic field motor functional MRI (3 Tesla)

in glioma patients by navigated electrocortical stimulation and postoperative outcome. J Neurol Neurosurg Psychiatry. 2005; 76:1152–1157. others. [PubMed: 16024896]

Ruge MI, Victor J, Hosain S, Correa DD, Relkin NR, Tabar V, Brennan C, Gutin PH, Hirsch J. Concordance between functional magnetic resonance imaging and intraoperative language mapping. Stereotact Funct Neurosurg. 1999; 72:95–102. [PubMed: 10853058]

Rumpel H, Chan LL, Tan JS, Ng IH, Lim WE. Clinical functional magnetic resonance imaging for pre-surgical planning--the Singapore General Hospital experience with the first 30 patients. Ann Acad Med Singapore. 2009; 38:782–786. [PubMed: 19816637]

Schlosser MJ, Luby M, Spencer DD, Awad IA, McCarthy G. Comparative localization of auditory comprehension by using functional magnetic resonance imaging and cortical stimulation. J Neurosurg. 1999; 91:626–635. [PubMed: 10507385]

Singh M, Wong CW. Independent component analysis-based multifiber streamline tractography of the human brain. Magn Reson Med. 2010; 64:1676–1684. [PubMed: 20882674]

von Stockhausen HM, Thiel A, Herholz K, Pietrzyk U. A convenient method for topographical localization of intracranial electrodes with MRI and a conventional radiograph. Neuroimage. 1997; 5:S514.

Wengenroth M, Blatow M, Guenther J, Akbar M, Tronnier VM, Stippich C. Diagnostic benefits of presurgical fMRI in patients with brain tumours in the primary sensorimotor cortex. Eur Radiol. 2011; 21:1517–1525. [PubMed: 21271252]

Wu HC, Nagasawa T, Brown EC, Juhasz C, Rothermel R, Hoechstetter K, Shah A, Mittal S, Fuerst D, Sood S. Gamma-oscillations modulated by picture naming and word reading: Intracranial recording in epileptic patients. Clin Neurophysiol. 2011; 122:1929–1942. others. [PubMed: 21498109]

Wyllie, E.; Awad, I. Invasive neurophysiologic techniques in the evaluation for epilepsy surgery in children.. In: Luders, HO., editor. Epilepsy Surgery. Raven Press; New York: 1991. p. 409-412.

Yeo BT, Sabuncu MR, Vercauteren T, Ayache N, Fischl B, Golland P. Spherical demons: fast diffeomorphic landmark-free surface registration. IEEE Trans Med Imaging. 2010; 29:650–668. [PubMed: 19709963]

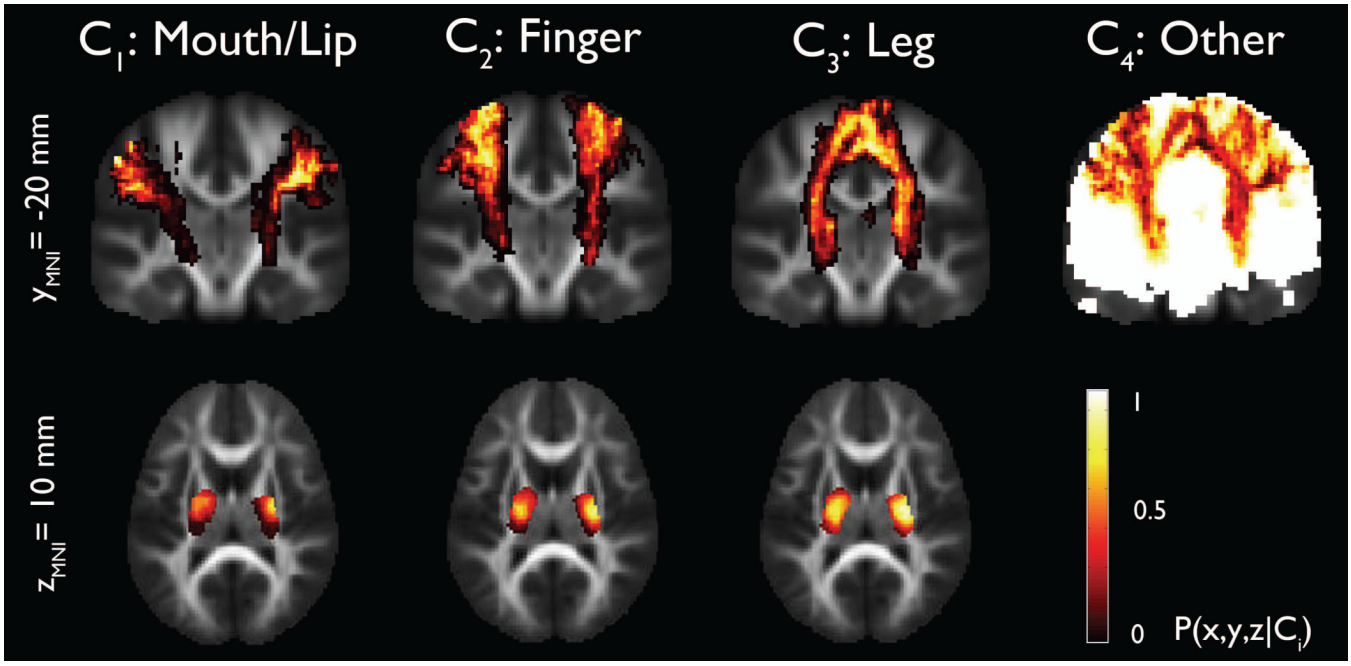

Figure 1.
Stereotaxic probability maps of “mouth/lip”, “fingers”, and “leg” pathways from the ICA +BSM tractography. Each map shows the probability of a voxel that belongs to mouth/lip, finger, and leg pathways in healthy children (n=17).

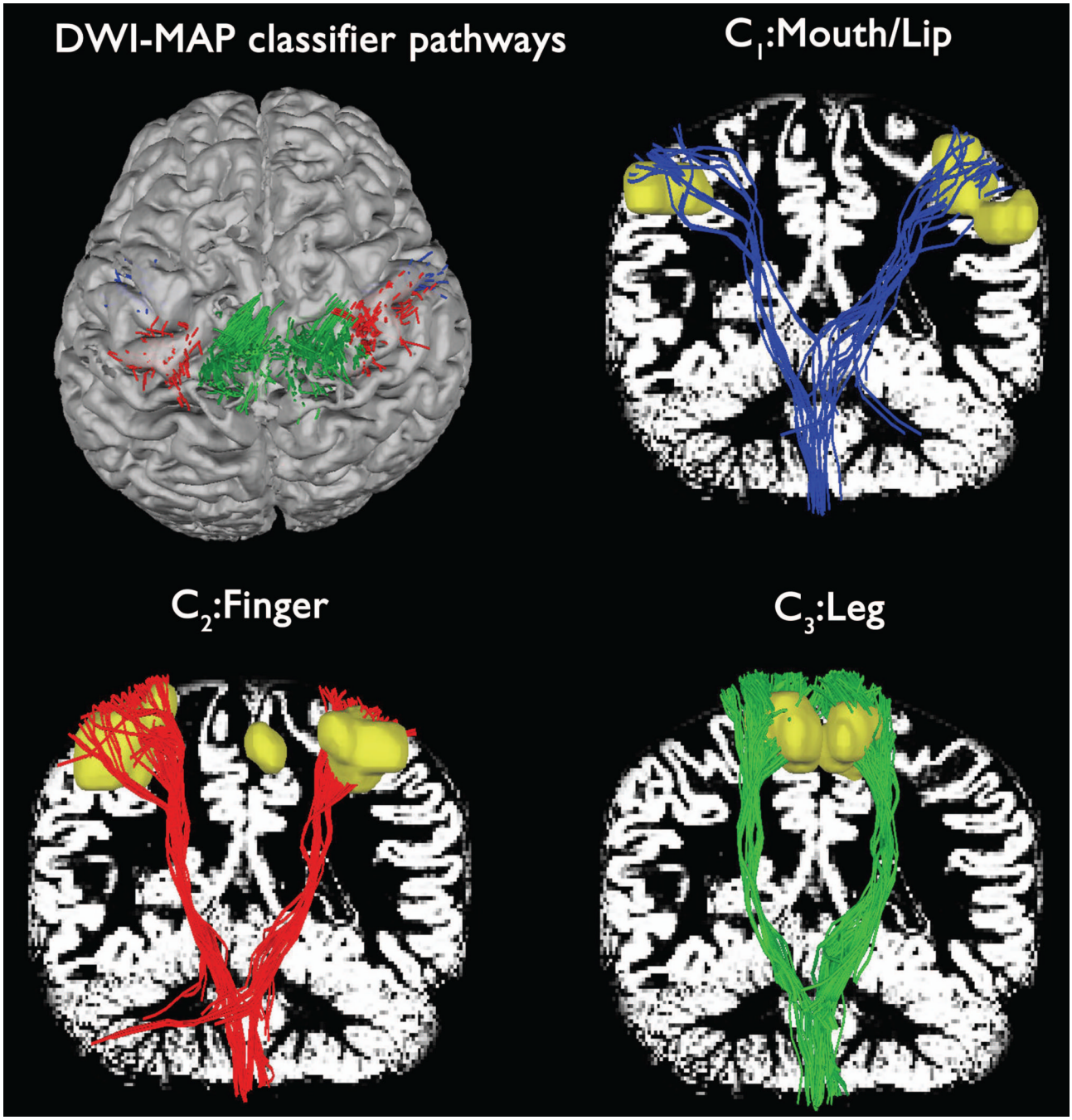

Figure 2.
Automatic detection of three pathways using the DWI-MAP classifier obtained from a normal participant. To demonstrate the reliability of the MAP classification, three pathways, C_1: mouth/lip (blue), C_2: finger (red), C_3: leg (green) were presented with corresponding fMRI activations (yellow clusters). White background shows gray matter map.

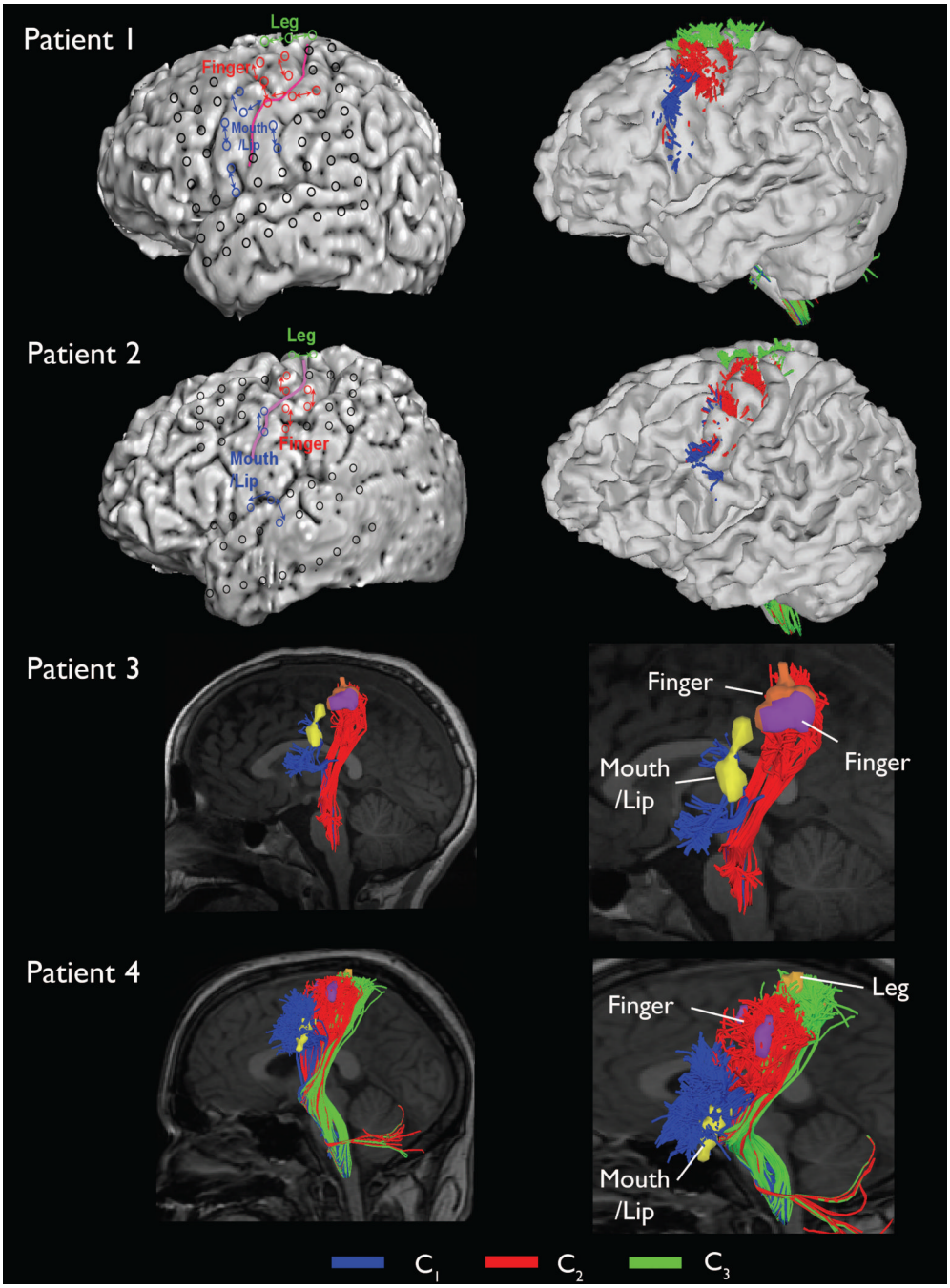

Figure 3.

Automatic detection of primary motor pathways using DWI-MAP classifier obtained from four patients with focal epilepsy. Black circles on the three dimensional brain surface represent the locations of electrodes used for ESM. C_1: 'mouth/lip pathway', C_2: 'finger pathway', C_3: 'leg pathway' were obtained using the DWI-MAP classifier.

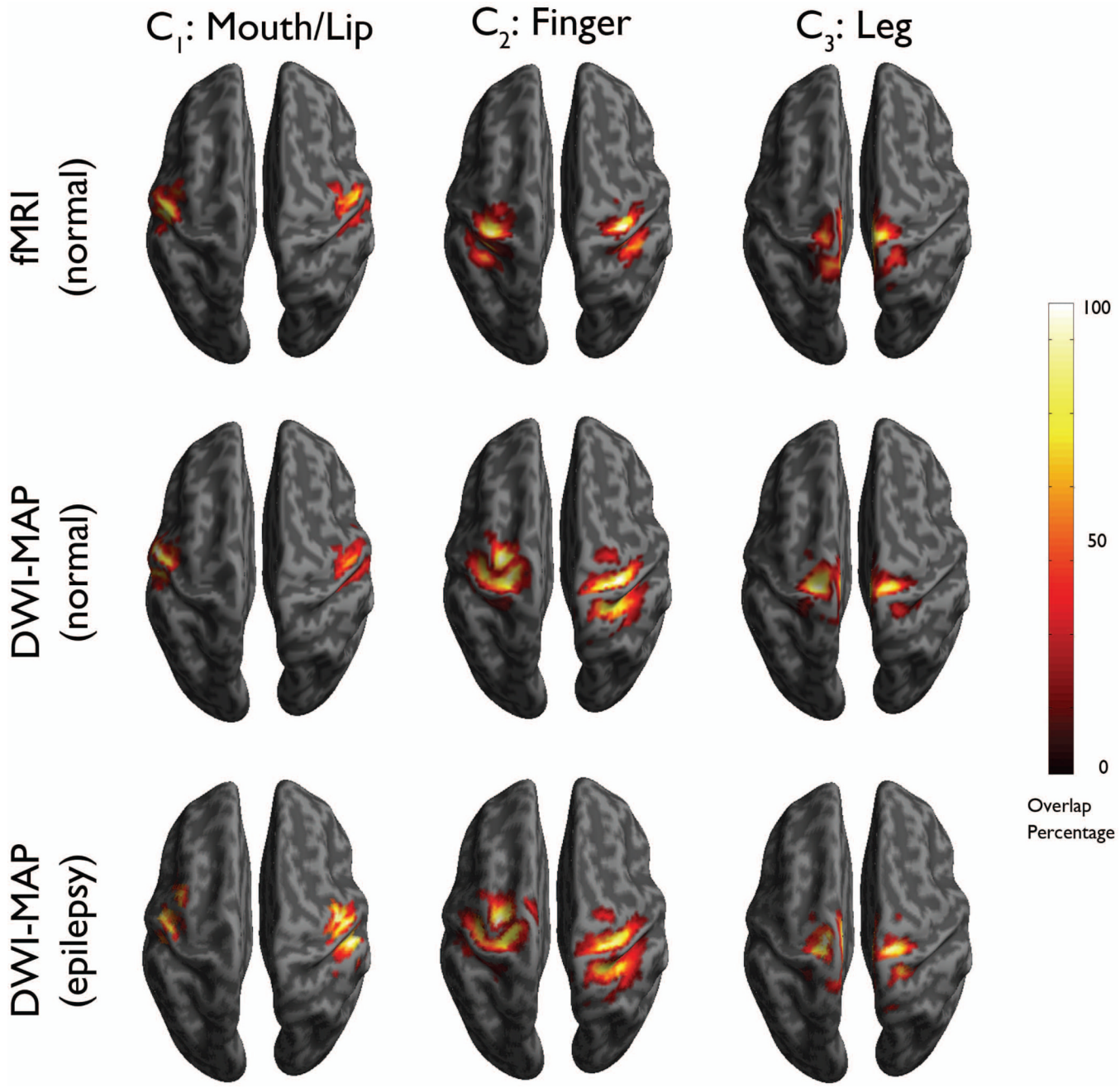

Figure 4.

Comparison of overlap percentage maps obtained from fMRI in healthy children (n=17, top), DWI-MAP classification in healthy children (n=17, middle), and DWI-MAP classification in children with epilepsy (n=20, bottom). Color bar indicates the overlap percentage of all cortical localizations obtained from each group.

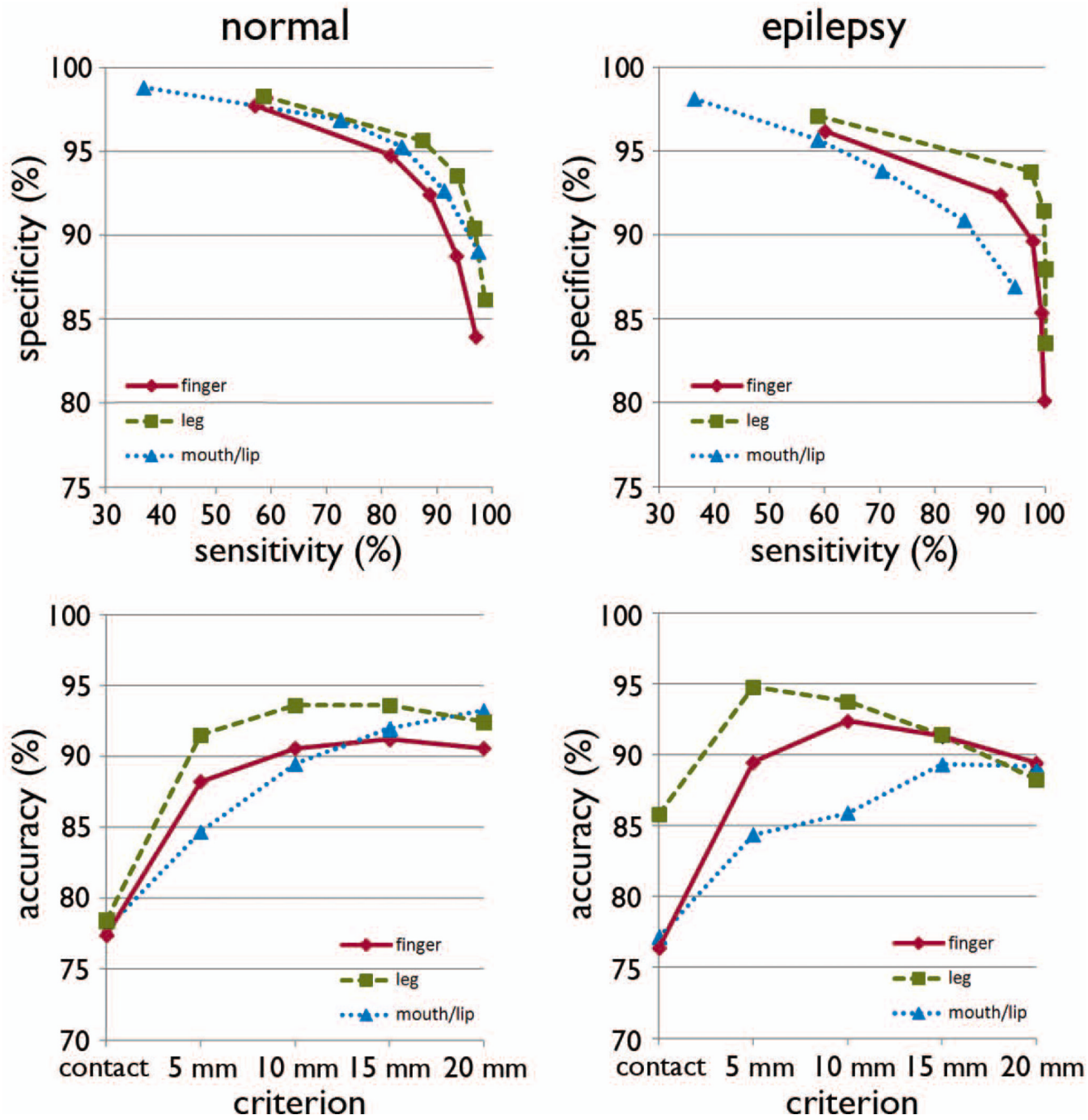

Figure 5.

Receiver operator curve analyses for the three pathways, C_1: mouth/lip, C_2: finger, and C_3: leg. For each of five separation criteria (contact, 5mm, 10mm, 15mm, 20mm), the group average of sensitivity, specificity, and accuracy was evaluated from normal children (n=17) and children with epilepsy (n=20).